Wave propagation in dissipative microstructured materials

Tarvo Sillat and Jüri Engelbrecht

Centre for Nonlinear Studies, Institute of Cybernetics at Tallinn Technical University, Akadeemia tee 21, 12618 Tallinn, Estonia; tarvo@ioc.ee, je@ioc.ee

Abstract. One-dimensional deformation waves in microstructured materials are described by an hierarchical evolution equation that clearly distinguishes macro- and microstructural behaviour. The pseudospectral method is used for numerical simulation supported by the analytical solution for the linear case. It is shown how dissipative effects on various scales affect the harmonic wave. The shock wave formation on macroscale is strongly influenced by the microstructure. The results of this study can be used for material processing.

Key words: wave hierarchy, dissipation, microstructure.

1. INTRODUCTION

The concept of microstructured materials is widely used in contemporary solid mechanics (cf. [1–4]). The corresponding theories describing the behaviour of solids take into account both the macroscopic and microscopic properties of materials, related to different length scales. Several mathematical models have been derived on that basis, accounting for possible dispersion and dissipation (eg. [4–6]). Among other methods, the formalism of internal variables has proved useful for describing the effects of microstructures with needed physical correctness [7]. From the viewpoint of wave motion, the implementation of ideas of internal variables has revealed an extremely important feature: it is possible to derive a mathematical model with clear distinction of scales in the material related to those of excitation (impact). For example, it has been shown [8] that a single evolution equation for 1D longitudinal waves can be derived involving two operators: one describing the propagation in the macrostructure, another – in the microstructure. The control parameter is the ratio of the length scale in the material to wavelength (or frequency) of the initial excitations. In [8], the

dissipative behaviour was studied, but the dispersive effects could also be described in a similar way (cf. [6]). Following [9], such mathematical models reflect wave hierarchy. On the basis of [8], more detailed analysis of dissipative effects was carried out in [10]. Here the results of this analysis are presented and discussed. It is shown that beside dissipative effects also the phase shift of a harmonic wave can occur due to the microstructure. It is also shown that the shock wave formation typical of the so-called Burgers model can be controlled by the microstructure.

Section 2 presents the mathematical model for describing the evolution of 1D longitudinal waves. In Section 3, the numerical method used in simulations is briefly explained. Section 4 is the focal point of the paper, where both analytical and numerical results are presented and analysed. The final Section 5 includes conclusions.

2. MATHEMATICAL MODEL

The mathematical model is based on the general balance laws of micro-structured solids [1] distinguishing between a gross structure (macroscopic) stress and force, and an interaction force between gross and fine structure. In general, for the gross structure we use the following notation: $\mathbf{S}$ is the first Piola–Kirchhoff stress tensor, $\mathbf{v} = \rho \dot{\mathbf{y}}$ the linear momentum, $\mathbf{b}_{\mathrm{mac}}$ the body macro-force, $\mathbf{k}$ the interactive microforce, $\mathbf{b}_{\mathrm{mic}}$ the body microforce, $\dot{\mathbf{y}}$ the macro-scopic velocity, $\mathbf{w} = \mathbf{I}_{\mathrm{in}} \, \delta$, where δ is the microstructural field, and $\mathbf{I}_{\mathrm{in}}$ is an "inertia" tensor. Then, for any region $W \subset B$ (B is a classical deformable body), with $\mathbf{n}$ being the outward unit normal to ∂W, we have

$$\int_{\partial W} \mathbf{S} \, \mathbf{n} \, da + \int_W \mathbf{b}_{\mathrm{mac}} dV = \frac{d}{dt} \int_W \mathbf{v} \, dV, \tag{2.1}$$

$$\int_W \mathbf{k} \, dV + \int_W \mathbf{b}_{\mathrm{mic}} dV = \frac{d}{dt} \int_W \mathbf{w} \, dV. \tag{2.2}$$

Further we neglect $\mathbf{b}_{\mathrm{mac}}$, $\mathbf{b}_{\mathrm{mic}}$, and take $\mathbf{I}_{\mathrm{in}} = 0$. This means that the micro-structural field δ is noninertial and can be treated as an internal variable [7]. In the 1D case the system (2.1), (2.2) yields

$$u_t = v_x, \quad v_t = \sigma_x, \quad 0 = k, \tag{2.3}$$

where $u(x, t) = y_x - 1$, $v = y_t$ and σ, k are the unidimensional counterparts of $\mathbf{S}$ and $\mathbf{k}$.

The governing equation is derived by using the free-energy function

$$F = F(u, d) = \frac{1}{2} c^2 (u - \lambda d)^2 + \varphi(d), \tag{2.4}$$

where d is the unidimensional counterpart of δ; c and λ are given constants, and $\varphi(d)$ is a given function (of order higher than two). In addition, the non-equilibrium fields $\hat{\sigma}$ and $\hat{k}$ of σ and k, respectively, are used [6]:

$$\sigma = \frac{\partial F}{\partial u} + \hat{\sigma}, \quad k = -\frac{\partial F}{\partial d} + \hat{k}, \tag{2.5}$$

with

$$\hat{\sigma} = Av_x + Bd_t, \quad \hat{k} = -Cv_x - E(d_t), \tag{2.6}$$

where A, B, C are constants and E is a certain function of its argument that determines the scale of the microstructure (the simplest case related to the derivative of $E(d_t)$, denoted by E_{dt}). The second important notion is the concept of internal variables. For detailed derivation of the governing equation the reader is referred to [6]. In dimensionless variables the final result is the following evolution equation in moving coordinates σ, ς:

$$\frac{\partial^2 \beta}{\partial \varsigma \partial \sigma} - K \frac{\partial^3 \beta}{\partial \varsigma^3} + Q \left[\left(\frac{\partial \beta}{\partial \varsigma} \right)^2 + \beta \frac{\partial^2 \beta}{\partial \varsigma^2} \right] + \lambda^2 L \left(\frac{\partial \beta}{\partial \sigma} + M \frac{\partial \beta}{\partial \varsigma} + \beta \frac{\partial \beta}{\partial \varsigma} - N \frac{\partial^2 \beta}{\partial \varsigma^2} \right) = 0. \tag{2.7}$$

Here the following notation is used. The field variable β is related to $u\,(u = \beta u_0)$, u_0 is the amplitude of the input, the moving coordinates are $\sigma = a_1 u_0 \tau \tau_c^{-1}$, $\tau = \varepsilon x$, $\varsigma = (ct - x)\tau_c^{-1}$ (a_1 is a relative nonlinear constant and τ_c – the wavelength of the input). The dimensionless constants reflect the macro- and microstructural properties of the material [8,10]. Leaving aside rather scrupulous formulae for constants, the following should be stressed. All the dimensionless constants, except Q ($Q = \operatorname{sign} m$) can be presented as a product of two parameters

$$P = HI, \tag{2.8}$$

where H is related to the material parameters and I – to the input parameters [8,11]. It means that the physical effects are controlled by properties of the material on one hand and the amplitude and the frequency (the wavelength) of the input on the other hand. The general structure of Eq. (2.7) reveals directly the hierarchical character of the wave propagation (cf. [9]). Namely, if $\lambda^2 L$ is small, then the second part of Eq. (2.7) (in round brackets) can be neglected and the wave propagation is affected only by the gross (macroscopic) structure. If, however, $\lambda^2 L$ is large, then the influence of the fine (microscopic) structure dominates over the macroscopic properties. Certainly, the intermediate scales are also of interest when both parts are present.

3. NUMERICAL ALGORITHM AND LINEAR SOLUTION

The pseudospectral method is used for the numerical simulation. However, in case of Eq. (2.7), the situation is more complicated than in the standard cases (cf. [12,13]) due to the existence of the mixed derivative $\partial^2 \beta / \partial\varsigma\partial\sigma$ parallel to $\partial\beta / \partial\sigma$. This has forced us to use a different approach from standard one. The algorithm is based on the following considerations.

Let the interval of interest be 2π and the grid formed by n points with $\Delta = 2\pi/n$. Then

$$\varsigma = \{\varsigma_i\} = \{i\Delta\}_{i=0}^{n-1} \tag{3.1}$$

and

$$U = \{U_i\} = \{u(i\Delta, \sigma)\}_{i=0}^{n-1}. \tag{3.2}$$

The discrete Fourier transform is defined by

$$U(\omega, \sigma) = Fu = \sum_{j=0}^{n-1} U_j e^{-2\pi i j\omega/n} \tag{3.3}$$

and the inverse discrete Fourier transform by

$$u(\varsigma, \sigma) = F^{-1}U = \sum_{\omega} U(\omega, \sigma) e^{-2\pi i j\omega/n}, \tag{3.4}$$

where i is the imaginary unit and

$$\omega = 0, \pm 1, \pm 2, \ldots, \pm(n/2 - 1), -n/2. \tag{3.5}$$

Now, for the derivatives we get:

$$U_\varsigma = \{u_\varsigma(i\Delta_\varsigma, \sigma)\}_{i=0}^{n-1} \approx F^{-1}(i\omega FU), \tag{3.6a}$$

$$U_{\varsigma\varsigma} = \{u_{\varsigma\varsigma}(i\Delta_\varsigma, \sigma)\}_{i=0}^{n-1} \approx -F^{-1}(\omega^2 FU), \tag{3.6b}$$

$$U_{\varsigma\varsigma\varsigma} = \{u_{\varsigma\varsigma\varsigma}(i\Delta_\varsigma, \sigma)\}_{i=0}^{n-1} \approx -F^{-1}(i\omega^3 FU). \tag{3.6c}$$

In this way we can handle the space derivatives and Eq. (2.7) can be written in the following form:

$$\frac{d}{d\sigma}U + \frac{d}{d\sigma}DU + K(DU, D^2U, D^3U) = 0, \tag{3.7}$$

where K is the linear or nonlinear function of the space derivatives and $\mathbf{D}$ is the differential operator

$$\mathbf{D}U = \mathrm{F}^{-1} i\omega \cdot \mathrm{F}U. \tag{3.8}$$

With a new variable

$$V = U + \mathbf{D}U \ \text{ or } \ V = \mathrm{F}^{-1}[(1 + i\omega)\,\mathrm{F}U] \tag{3.9}$$

and the inverse transform

$$U = \mathrm{F}^{-1}\left[\frac{1}{1 + i\omega}\,\mathrm{F}V\right], \tag{3.10}$$

we obtain the formula for space derivatives

$$\mathbf{D}^n U = \mathrm{F}^{-1}\frac{(i\omega)^n}{1 + i\omega}\,\mathrm{F}V. \tag{3.11}$$

In this way, Eq. (3.7) is transformed into the ordinary differential equation with respect to V :

$$\frac{d}{d\sigma}V + K\left(\mathrm{F}^{-1}\frac{i\omega}{1 + i\omega}\,\mathrm{F}V, \ldots\right) = 0. \tag{3.12}$$

For Eq. (3.12), several Runge–Kutta algorithms were employed. The crucial point is that Eq. (2.7) is not conservative and the conservation laws as usual KdV-type calculations could not be used. Different time and space steps were tested in various solvers and results were compared also with the known linear solution (see below). In Section 4, the number of grid points $n = 128$ and the time step satisfying $h < 3(\Delta\varsigma)^3 / (2\pi^2)$ with the fourth-order Runge–Kutta integration scheme were used.

In the linearized case (the geometrical and physical nonlinearities neglected), the solution of the governing equation derived from Eq. (2.7) can be sought in the form of a superposition of different Fourier components:

$$\beta = \beta_0 \exp[i(k\varsigma - \omega\sigma)], \tag{3.13}$$

where k is the wave number and ω the frequency. The corresponding dispersion relation is then

$$\omega = [A(k) - B(k)]C(k),$$

$$A(k) = k^3 \lambda^2 LK + k\lambda^4 L^2 M - \lambda^2 LNk^3,$$

$$B(k) = Kk^4 + \lambda^2 LMk^2 + k^2\lambda^4 L^2 N, \tag{3.14}$$

$$C(k) = (k^2 - \lambda^4 L^2)^{-1}.$$

Beside the full solution

$$\beta \sim \exp[-B(k)C(k)\sigma]\,\exp[i\,(k\varsigma - A(k)C(k)\sigma)], \qquad (3.15)$$

we are interested in its approximations for λ small

$$\beta \sim \exp[-Kk^2\sigma]\,\exp[i\,k\varsigma] \qquad (3.16)$$

and for λ large

$$\beta \sim \exp[-kN\sigma]\,\exp[i\,(k\varsigma - kM\sigma)]. \qquad (3.17)$$

In the case of the input $\beta = \sin\varsigma$, the phase velocity v_{ph} is

$$v_{ph} = (\lambda^2 LK + \lambda^4 L^2 M - \lambda^2 LN)(1 + \lambda^4 L^2)^{-1}. \qquad (3.18)$$

Clearly, the linear solution already gives valuable information. It was shown already in [8] that for the given model both the gross and fine structures are dissipative but with different dissipation rates. In Eq. (2.7) it is emphasized by parameters K and N, respectively.

4. ANALYSIS AND DISCUSSION

To the knowledge of the authors, no sufficient experimental values of parameters exist for Eq. (2.7). Therefore, here the aim was set up to analyse the limit cases and understand the influence of all parameters on the distortion of an initial harmonic excitation $\beta(0,\varsigma) = \sin\varsigma$. The numerical simulation together with linearized solution was used.

First, some typical time slice plots are shown in Fig. 1 (linear model) and Figs. 2, 3 (nonlinear model). The effects easily understood in all simulations are the attenuation and phase shifts. Due to the complicated structure of the governing equation, these effects can also be coupled for intermediate values of λ^2. For such an analysis we have used the linear model, while the nonlinear model reveals then the possible changes in shock wave formation.

In linear analysis the solutions of Eq. (2.7) are shown for different λ^2 values (Fig. 1c–e), with all the other parameters taken equal to one (all terms in this equation are taken into account equally). For comparison, the macroequation (Fig. 1a) and microequation (Fig. 1b) are solved using the same parameter selection. The intermediate region for λ^2 is evidenced by stronger attenuation of the wave profile around $\lambda^2 = 1$ than in the cases where either the macro- or microstructure was only taken into account. As is seen in Fig. 4, where the amplitude of β (at $\sigma = 1$) at different λ values is shown, the wave amplitude at small λ values is determined by the macrodissipation parameter K, and the wave amplitude at large λ is determined by the microdissipation parameter N. However, in the intermediate region the amplitude is mainly dependent on the

108
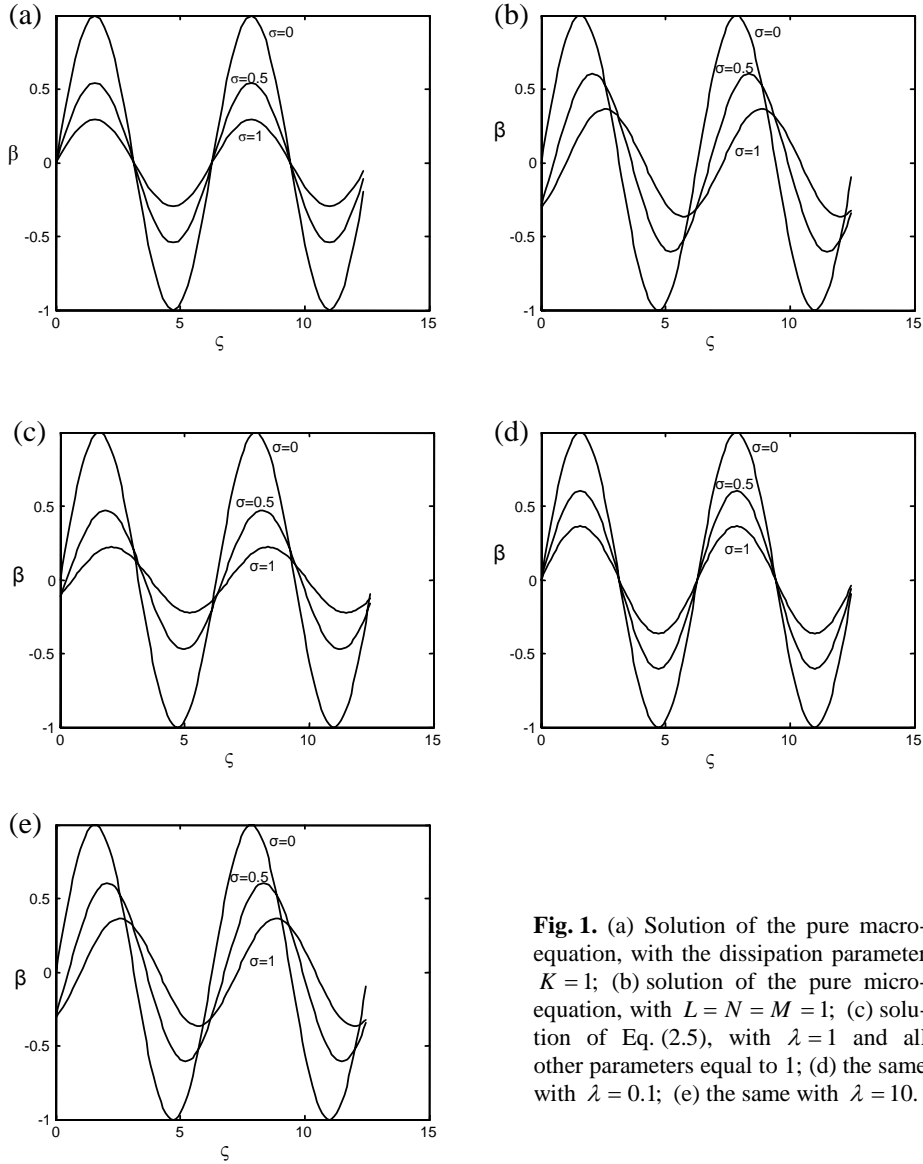
Fig. 1. (a) Solution of the pure macro-equation, with the dissipation parameter $K = 1$; (b) solution of the pure micro-equation, with $L = N = M = 1$; (c) solution of Eq. (2.5), with $\lambda = 1$ and all other parameters equal to 1; (d) the same with $\lambda = 0.1$; (e) the same with $\lambda = 10$.

parameter M. Also the phase shift (phase velocity) changes with increasing λ^2 starting from a pure macrostructural case, where no phase shift is present, and ending with a pure microstructural case, where the phase shift (velocity) is determined by the parameter M, passing the intermediate region, where phase velocity could be even higher than in the pure microstructural case (see Eq. (3.17) and Fig. 5). Like in the case with the amplitude, it seems that in the intermediate region the parameters that in marginal cases are "dissipative" – K and N (not M) – are causing the phase shift. However, K brings about changes in phase velocity in positive direction, N in negative direction. In this

109
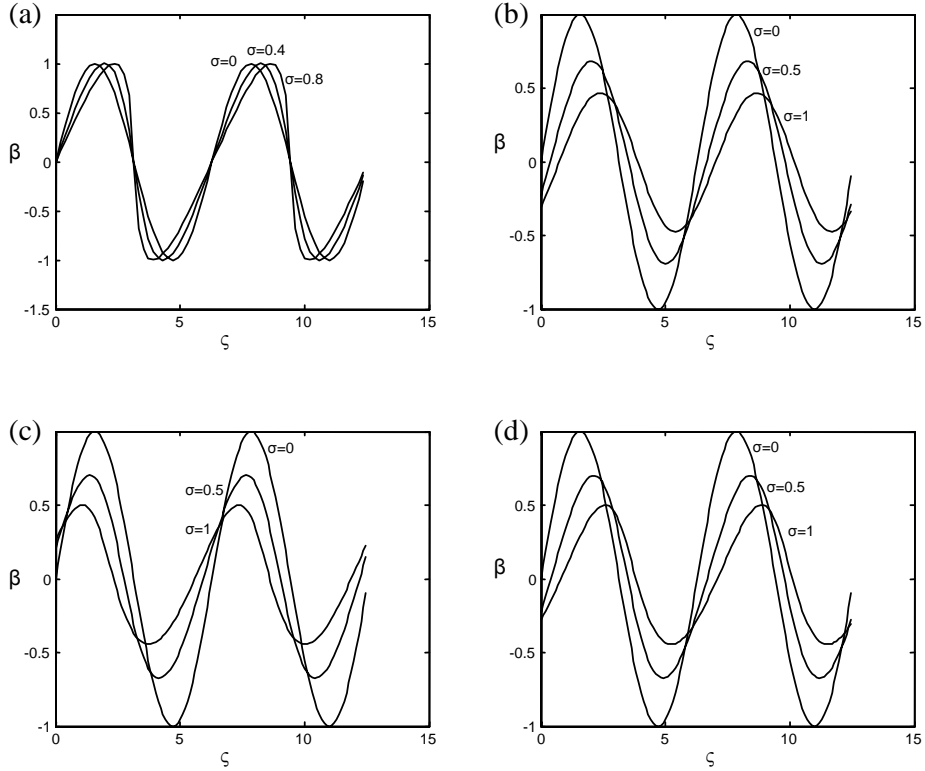
Fig. 2. (a) Solution of Eq. (2.5), with $Q = R = \lambda^2 L = 1$, all other parameters neglected; (b) solution of Eq. (2.5), with $K = \lambda^2 L = R = Q = 1$, other parameters equal to zero, i.e. macrodissipation avoids shock wave formation due to nonlinearity; (c) solution of Eq. (2.5), with $\lambda^2 L = R = Q = 1$, $N = 3$, other parameters equal to zero; (d) solution of Eq. (2.5), with $\lambda^2 L = Q = R = 1$, $M = 3$, other parameters equal to zero, i.e. nonlinearity with microdissipation.

way the wave hierarchy associated with changing λ^2 is reflected also in the function of parameters. For example, with small λ^2 the parameter K causes dissipation; with increase in λ^2 it starts to cause mainly the phase shift; with further increase in λ^2 the influence of K on the wave profile will gradually disappear. Similar hierarchy is also evident with M and N.

Now the influence of the parameter L is considered. In principle, L compares the input wavelength (τ_c) with the characteristics of the micro-structure (E_{dt}) (for details see [8]). Numerical calculations revealed that changes in L, both increasing and decreasing, do not change the wave profile if all other parameters are zero. Physically it means that the wave process "feels" both the micro- and macrostructure, but there is no dissipation or phase shift. Although we have kept λ and L separated from Eq. (2.7), it is clear that it is not only λ, but the product of λ^2 and L that determines the hierarchy, and instead of two microstructural parameters λ and E_{dt}, we could speak of λ^2 / E_{dt} as one microstructural parameter in terms of wave profile changes.

110

(a)   (b)

(c)   (d)
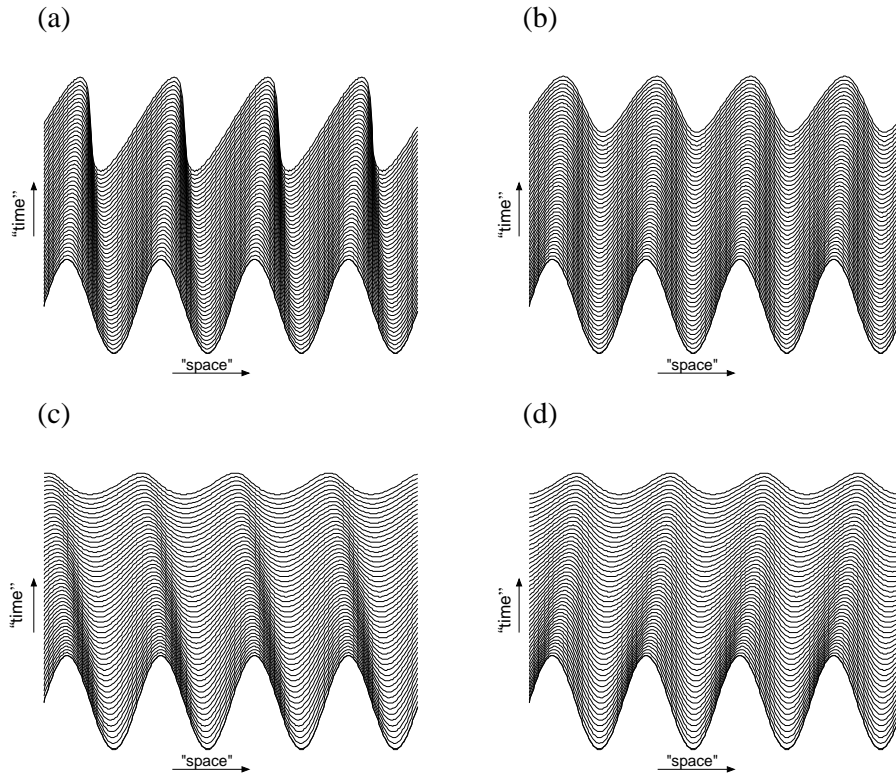
Fig. 3. Same solutions as in Fig. 2, but instead of certain time slices, the whole time-slice plots are shown.

In conclusion, these results show that if both terms $\partial^2(...)/\partial\sigma\partial\varsigma$ and $\partial(...)/\partial\sigma$ are taken into account, then the parameters L, M, and N (that are intimately connected to the properties of the microstructure) cause the change in the macrowave profile (it is especially clear when we take the macrodissipation equal to zero). In this way, if it is possible to relate E_{dt} and other characteristics of the microstructure to the real materials, one could use these results and knowledge of material processing in order to change the characteristics of wave propagation in a desired way by changing the properties of materials microstructure. Also parameters that in pure macroscopic or pure microscopic models act only with one function: either connected to attenuation or phase shift, might cause both effects in the intermediate region.

If only nonlinear terms were included, the shock wave (N-wave) would form (see Figs. 2a, 3a). We tried to understand how the shock formation was related to the material properties of different scales. For that we introduced different parameters separately while being in the intermediate region $\lambda^2 L = 1$ where the
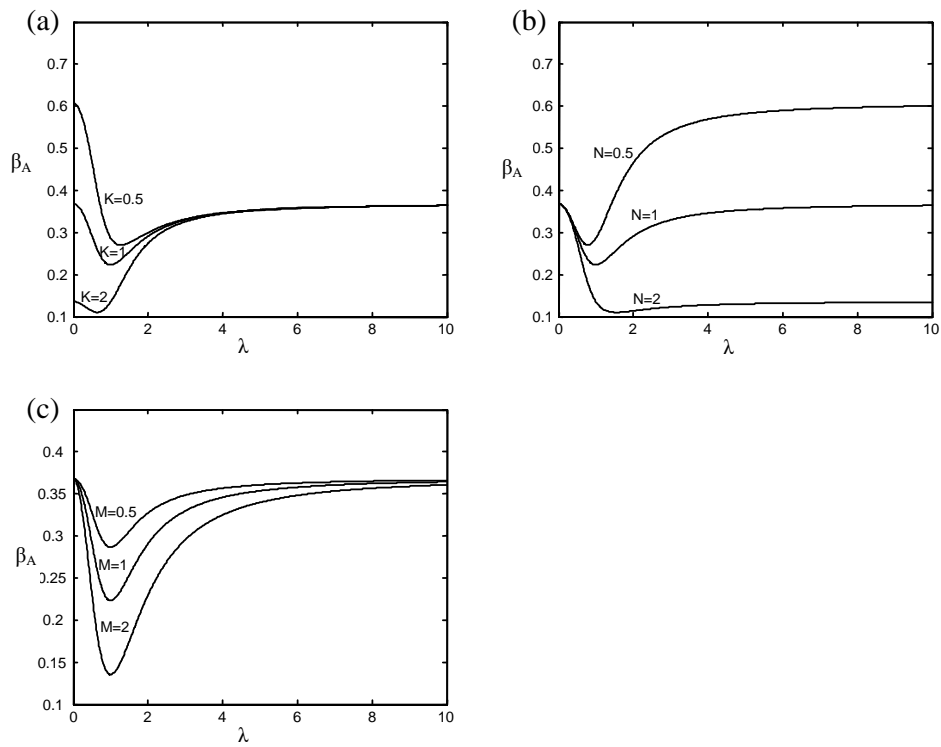
Fig. 4. Amplitude of β at $\sigma = 1$, calculated with linear model: one parameter is varied and others are taken equal to 1. (a) Influence of K, with $N = M = L = 1$; (b) influence of N; (c) influence of M.
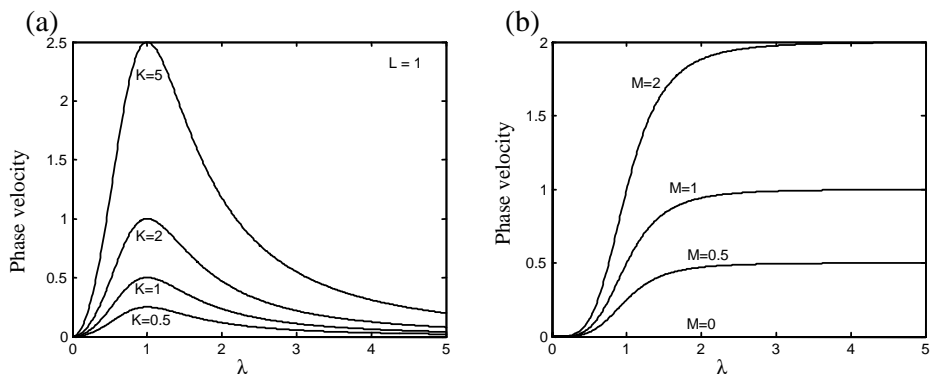
Fig. 5. Influence of parameters on phase velocity: (a) influence of K, with $L = 1$, $M = N = 0$; (b) influence of M, with $L = 1$, $K = N = 0$.

112

influences of both the macro- and microstructure should be evident. If a pure macroequation is solved, it is known that dissipation due to K withdraws the shock formation. The parameter K has the same effect in the intermediate region (Figs. 2b, 3b). Note also the phase shift that agrees well with the linear analysis. On the other hand, shock wave formation is clearly influenced by the presence of the microstructure (Figs. 2c,d and 3c,d). Both N and M are capable of eliminating the shock wave formation in macroscale. In this way, in principle, it is possible by changing the microstructure of the material to avoid the shock wave formation due to the nonlinear properties of the material. The nonlinear effects need certainly further studies, especially with other values of $\lambda^2 L$. Due to combined influence of macro- and microstructure (different terms in Eq. (2.7)), the dispersive effects could also be evident.

5. CONCLUSIONS

We have studied numerically a certain one-dimensional evolution equation derived for microstructured solids. Theoretically it has been guessed earlier that this equation contains parameters that cause dissipation and phase shift (and in the nonlinear case the nonlinear behaviour) [8]. It seems to be specific to materials with the microstructure that it is not possible to distinguish a parameter that has only a dissipative or phase shift effect. The reason for such a conclusion is the existence of two different mechanisms modelled by two different terms containing derivatives taken with respect to "time" variable. In nonlinear cases the macroscopic and microscopic nonlinearities cause the formation of a classical N-wave, which is widely known. However, it is shown that the shock wave formation can be principally avoided by changing parameters in different scales. This knowledge about the influence of the material properties on wave propagation can be used for material processing. Nevertheless, several questions remain open for further research. As the parameters of the wave equation depend also on input, different input waves should be studied (e.g. the influence of the frequency should be analysed). In this way it is possible to study further the interplay and dependence between different parameters and their physical and input characteristics (see (2.8)). The problem is that not all independent changes in parameter values used in this work may be physically allowed. Also, the connection between the parameters of this model and the properties of the real materials needs future research.

ACKNOWLEDGEMENTS

REFERENCES

1. Capriz, G. *Continua with Microstructure*. Springer, New York, 1989.
2. Suquet, P. (ed.). *Continuum Micromechanics*. Springer, Wien, 1997.
3. Sih, G. G. (ed.). *Mesomechanics 2000*, Vols. I, II. Tsinghua University Press, Beijing, 2000.
4. Engelbrecht, J. and Braun, M. Nonlinear waves in nonlocal media. *Appl. Mech. Rev.*, 1998, **51**, 475–488.
5. Erofeev, V. I. and Potapov, A. I. Longitudinal strain waves in non-linearly elastic media with couple stresses. *Int. J. Non-Lin. Mech.*, 1993, **28**, 483–488.
6. Giovine, P. and Oliveri, F. Dynamics and wave propagation in dilatant granular materials. *Meccanica*, 1995, **30**, 341–357.
7. Maugin, G. A. and Muschik, W. Thermodynamics with internal variables. *J. Nonequilib. Thermodyn.*, 1994, **19**, 217–249 (Part I), 250–289 (Part II).
8. Engelbrecht, J., Cermelli, P. and Pastrone, F. Wave hierarchy in microstructured solids. In *Geometry, Continua & Microstructure* (Maugin, G. A., ed.). Hermann, Paris, 1999, 99–111.
9. Whitham, G. B. *Linear and Nonlinear Waves*. J. Wiley, New York, 1983.
10. Sillat, T. Wave propagation in dissipative microstructured materials. MSc thesis, Tallinn Technical University, 1997.
11. Engelbrecht, J. *Nonlinear Wave Processes of Deformation in Solids*. Pitman, London, 1983.
12. Salupere, A. On the application of the pseudospectral method for solving the Korteweg–de Vries equation. *Proc. Estonian Acad. Sci. Phys. Math.*, 1995, **44**, 73–87.
13. Peipman, T. and Engelbrecht, J. Two dimensional evolution equations of transient waves – an algorithm analysis by means of Fourier transform. *Acta Comment. Univ. Tartuensis*, 1982, 627, 107–112 (in Russian).

Lainelevi dissipatiivsetes mikrostruktuuriga materjalides

Tarvo Sillat ja Jüri Engelbrecht

Ühemõõtmelise lainelevi kirjeldamiseks on kasutatud varem tuletatud hierarhilist evolutsioonivõrrandit, milles on struktureeritult eraldatud makro- ja mikroefektid. Üldjuhul on laineväli leitud numbriliselt pseudospektraalmeetodit kasutades, kuid mittelineaarsete efektide hülgamisel on võrdluseks leitud ka analüütiline lahend koos vastava dispersiooniseadusega. On tuvastatud dissipatsiooniefektide mõju harmoonilisele lainele sõltuvalt koormusparameetritest ja mikrostruktuuri iseloomust. Olulised on seejuures ka võimalikud faasimuutused, mis kaasnevad amplituudi sumbumisega. On näidatud, milline on mikrostruktuuri mõju lööklaine tekkimisele makrotasandil. Tulemused loovad aluse mikrostruktuuriga materjalide paremaks sünteesiks.